

Two massive, rapid releases of carbon during the onset of the Palaeocene–Eocene thermal maximum

Gabriel J. Bowen^{1,2*}, Bianca J. Maibauer^{1,2}, Mary J. Kraus³, Ursula Röhl⁴, Thomas Westerhold⁴, Amy Steimke¹, Philip D. Gingerich⁵, Scott L. Wing⁶ and William C. Clyde⁷

The Earth's climate abruptly warmed by 5–8 °C during the Palaeocene–Eocene thermal maximum (PETM), about 55.5 million years ago^{1,2}. This warming was associated with a massive addition of carbon to the ocean–atmosphere system, but estimates of the Earth system response to this perturbation are complicated by widely varying estimates of the duration of carbon release, which range from less than a year to tens of thousands of years. In addition the source of the carbon, and whether it was released as a single injection or in several pulses, remains the subject of debate^{2–4}. Here we present a new high-resolution carbon isotope record from terrestrial deposits in the Bighorn Basin (Wyoming, USA) spanning the PETM, and interpret the record using a carbon-cycle box model of the ocean–atmosphere–biosphere system. Our record shows that the beginning of the PETM is characterized by not one but two distinct carbon release events, separated by a recovery to background values. To reproduce this pattern, our model requires two discrete pulses of carbon released directly to the atmosphere, at average rates exceeding 0.9 Pg C yr⁻¹, with the first pulse lasting fewer than 2,000 years. We thus conclude that the PETM involved one or more reservoirs capable of repeated, catastrophic carbon release, and that rates of carbon release during the PETM were more similar to those associated with modern anthropogenic emissions⁵ than previously suggested^{3,4}.

Global climate warming from the late Palaeocene through early Eocene was punctuated by several transient hyperthermal events². The most prominent of these events, the PETM, was characterized by a 5–8 °C temperature increase, a 3–6‰ negative carbon isotope excursion (CIE), and profound shifts in biotic communities². The PETM CIE reflects a massive release of ¹³C-depleted carbon to the ocean–atmosphere system at the event's onset. The source(s) and mechanism(s) of carbon release remain controversial, with hypotheses including thermal dissociation of marine methane hydrates, widespread oxidation of organic carbon, igneous intrusion into organic-rich sediments, and bolide impact². Improved constraints on the pattern and pace of PETM carbon-cycle change, particularly during the event's onset, are needed to further evaluate these mechanisms. However, recent publications paint widely divergent pictures of the CIE onset, ranging from slow, protracted (20,000 year) carbon release⁴ to a single, massive sub-decadal carbon burst³.

We recovered new sedimentological and isotopic records from approximately 375 m of strata spanning the Palaeocene–Eocene boundary in two boreholes at Polecat Bench (PCB, Bighorn Basin, Wyoming; Fig. 1) as part of the Bighorn Basin Coring Project (BBCP). Fluvial deposits of the Willwood Formation, which contains the PETM at this site, consist of mudrocks with moderate to strong pedogenic overprinting, heterolithic deposits with weak pedogenic overprinting, and channel and sheet sandstones⁶ (Fig. 1). Authigenic palaeosol carbonate is present as semi-rounded, grey to brown-grey, well-cemented nodules within pedogenically modified deposits. Carbonate nodules were sampled at 250 stratigraphic horizons in cores from both holes (Supplementary Information).

Carbon in pedogenic carbonate is derived from soil gas, which is a mixture of ¹³C-enriched atmospheric and ¹³C-depleted organic-respired CO₂. Data from modern soils and from other PETM records show that δ¹³C values of soil carbonate faithfully record changes in the isotopic composition of atmospheric CO₂ (refs 7,8). Pedogenic carbonate nodules are unlikely to record variations in atmospheric δ¹³CO₂ at centennial or shorter timescales because they take centuries to millennia to form in the soil⁸. A great advantage of pedogenic carbonate records, however, is that they are unlikely to be mixed or time-averaged over longer timescales, as are many other records^{9–11}.

Isotopic records from pedogenic carbonate in the two BBCP cores show excellent agreement with one another, and the new records are concordant with previously published data from nearby PCB outcrops⁷. The most prominent feature common to all records is the PETM CIE, which occurs between 118 and 55 m composite depth (MCD) in the BBCP record. The new data greatly increase the length and resolution of the δ¹³C record through the interval preceding the PETM, and include data from stratigraphic intervals never sampled in outcrop. The BBCP record suggests that mean δ¹³C values in ancient Polecat Bench soils were relatively stable through most of the latest Palaeocene, but shifted ~1‰ lower during the 15 m (≈37.5 kyr based on long-term accumulation rates of 0.4 m kyr⁻¹ (ref. 12)) preceding the CIE onset (Fig. 1). This pattern, which is similar to that observed in many marine records¹³, suggests a coupled shift in ocean/atmosphere δ¹³C values before the PETM, perhaps indicating destabilization of global carbon cycling in association with pre-PETM climate warming^{14,15} documented over similar timescales.

¹Department of Geology and Geophysics, University of Utah, Salt Lake City, Utah 84112, USA. ²Global Change and Sustainability Center, University of Utah, Salt Lake City, Utah 84112, USA. ³Department of Geological Sciences, University of Colorado, Boulder, Colorado 80309, USA. ⁴MARUM-Center for Marine Environmental Sciences, University of Bremen, Leobener Strasse, 28359 Bremen, Germany. ⁵Department of Earth and Environmental Sciences, University of Michigan, Ann Arbor, Michigan 48109, USA. ⁶Department of Paleobiology, Smithsonian Institution, Washington DC 20560, USA. ⁷Department of Earth Sciences, University of New Hampshire, Durham, New Hampshire 03824, USA. *e-mail: gabe.bowen@utah.edu

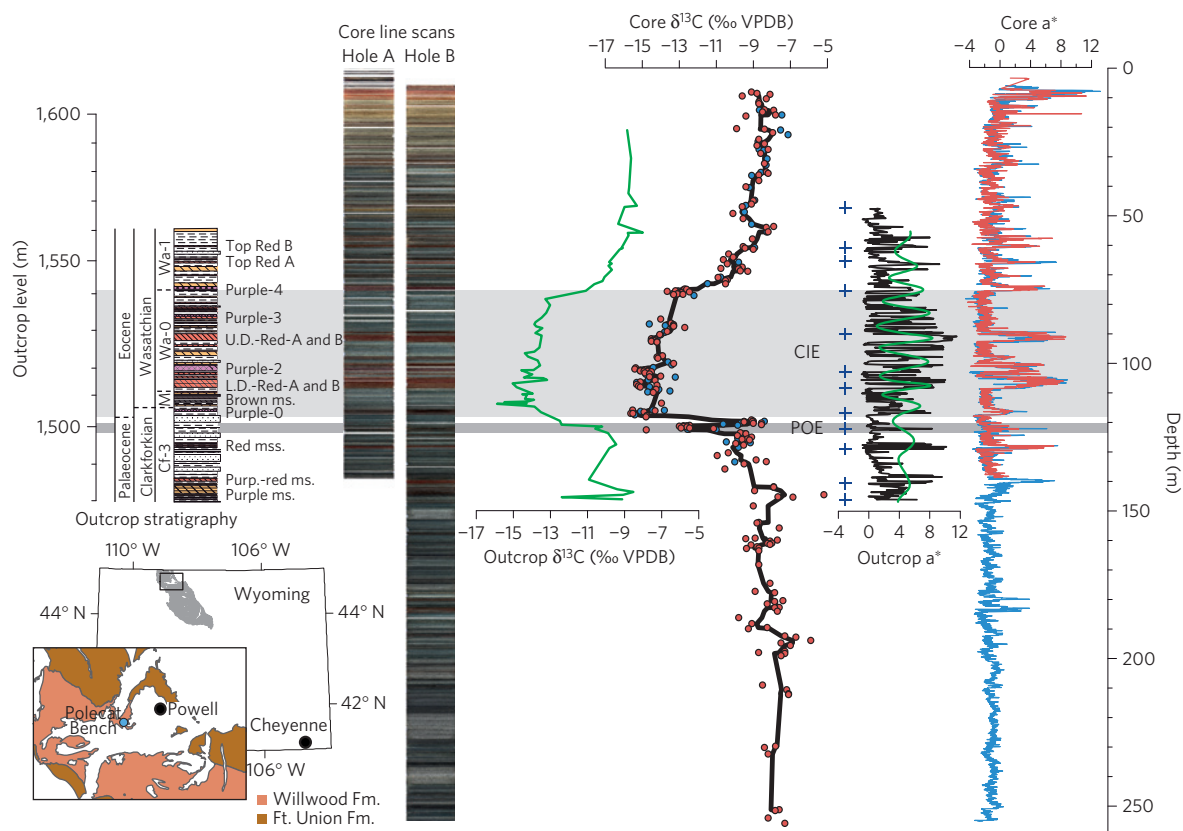


Figure 1 | Core and outcrop records of the PETM, Polecat Bench, Wyoming. Left to right: Litho-, bio- and chronostratigraphy from outcrop²⁹ (location maps inset); core line scan images; pedogenic carbonate $\delta^{13}\text{C}$ from outcrop⁷; pedogenic carbonate $\delta^{13}\text{C}$ from cores (blue symbols: hole A; red symbols: hole B; black line: 5-point moving average of both); redness index (a^*) for outcrop (green curve: 7.7 m Gaussian filter³⁰; blue crosses: outcrop to core tie points); a^* for cores (blue: hole A; red: hole B). Light grey box delineates the body of the CIE; dark grey highlights the pre-onset $\delta^{13}\text{C}$ excursion (POE). ms.: mudstone; mss.: mudstones; VPDB: Vienna Pee Dee Belemnite.

The most striking feature of our high-resolution record, however, is the presence of at least two discrete, negative $\delta^{13}\text{C}$ events within the PETM onset (Fig. 2). The older of these, which we here term the pre-onset excursion (POE), is a previously unrecognized -3‰ shift occurring abruptly between 123.6 and 122.6 MCD. Low POE values persist through $\sim 1.5\text{ m}$, above which nodule $\delta^{13}\text{C}$ values return to pre-POE values within 1.6 m of weakly pedogenically modified sediment deposited before the onset of the CIE. The POE and the recovery thereafter are stratigraphically coherent, of high amplitude relative to background $\delta^{13}\text{C}$ variation, each span several lithological and pedological units, and are recorded in nodules that clearly formed *in situ* (Fig. 2 and Supplementary Information). On the basis of these observations we infer that, like the main CIE, the POE reflects temporal changes in the $\delta^{13}\text{C}$ values of palaeosol CO_2 driven mainly by changes in the $\delta^{13}\text{C}$ value of atmospheric CO_2 . Lithological correlations indicate that the POE corresponds to a cluster of intermediate carbon isotope values in the outcrop record, and that the POE recovery falls within a 2.7-m interval not sampled in outcrop (Supplementary Fig. 4). Thus, the PCB outcrop data partially record the pattern of $\delta^{13}\text{C}$ change through the POE, which is expressed in more detail in the cores. A subsequent 5.7‰ $\delta^{13}\text{C}$ decline, reflecting the onset of the main CIE, occurs between samples collected at 119.26 and 118.19 MCD, in the same lithostratigraphic position as recorded in outcrop.

The negative $\delta^{13}\text{C}$ shifts that characterize the POE and CIE onsets each occur at the transition from one lithological unit to the next, with no intermediate $\delta^{13}\text{C}$ values and no indication of erosional truncation (Fig. 2 and Supplementary Information). However, each is associated with a gap in the stratigraphic distribution of carbonate nodules, suggesting a potential discontinuity in our records at

the onset of these events. To constrain the timing and pace of $\delta^{13}\text{C}$ change through the events we developed age models that assign time to individual lithological and pedological units based on thickness, sediment type and palaeosol maturity (Fig. 3 and Supplementary Fig. 11). These models provide a rigorous basis for interpreting our record because they account for known variations in short-term sediment accumulation rates. Given uncertainties in the model parameter values, however, and because the timing of nodule growth during soil formation is unknown, we use a range of age models and assumptions about the timing of nodule formation to evaluate possible interpretations of the record (Supplementary Information). These models suggest that the duration of the POE was between 2 and 5.5 kyr, with the onsets of the POE and CIE (the intervals of $\delta^{13}\text{C}$ decline) each lasting no more than ~ 1.5 kyr.

We use a global ocean–atmosphere–biosphere carbon-cycle box model that includes effects of temperature, atmospheric P_{CO_2} and soil respiration on pedogenic carbon isotopes (Supplementary Information) to identify scenarios of ^{13}C -depleted carbon release that are consistent with our observations. Scenarios that reproduce the excursion–recovery–excursion pattern seen in the BBCP record require two discrete episodes of carbon release directly to the atmosphere, with peak rates of release $>0.9\text{ Pg yr}^{-1}$ during each $\delta^{13}\text{C}$ excursion (Fig. 3 and Supplementary Fig. 13b,e). The model suggests that, in systems where the sedimentary record is time-averaged (for example, through bioturbation) or incompletely sampled, this C release is recorded as a two-step change without significant recovery. There is some evidence for a two-stage release with recovery from marine-margin records¹⁶, and our time-averaged model closely

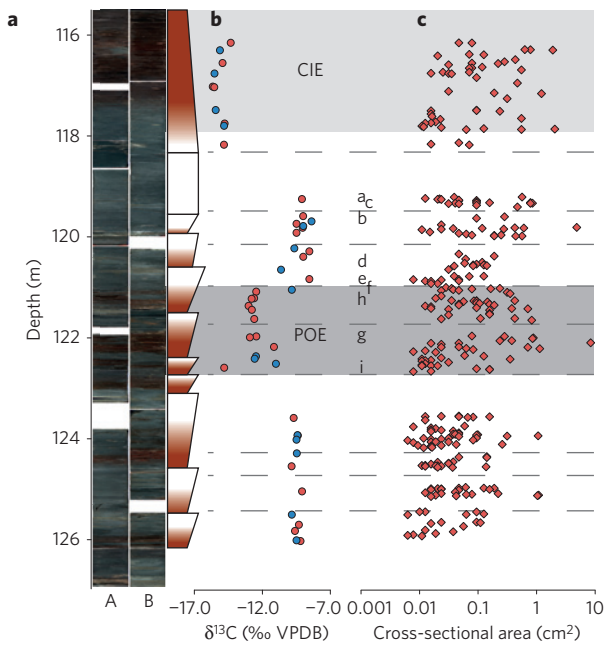


Figure 2 | Detailed stratigraphy, PETM onset interval. **a**, Linescan images for holes A and B with column showing grain size (width) and colour indicators of palaeosol B horizons. **b**, $\delta^{13}\text{C}$ of pedogenic carbonate nodules from holes A (blue) and B (red). **c**, Carbonate nodules in the cut face of hole B cores. Area was calculated from major and minor axis measurements, assuming an ellipsoidal geometry. Dashed lines show zones of genetically related carbonate nodules inferred from lithology and discontinuities in the stratigraphic distribution and size of nodules. Letters between **b** and **c** indicate positions of the nodules shown in Supplementary Fig. 6.

matches the pattern observed in many other marine records (for example, refs 7,15,17,18 and Fig. 3c).

The model is able to qualitatively represent the $\delta^{13}\text{C}$ recovery between the POE and CIE, driven mainly by mixing of the added carbon into the deep ocean, but produces a significant recovery only in scenarios with a short POE duration (~ 2 kyr), carbon injection into the atmosphere, and relatively slow surface-deep ocean mixing

(Fig. 3 and Supplementary Fig. 13 and Table 7). These results may suggest that our age models overestimate the duration of the POE and that the event involved less total carbon addition, at higher rates and over a shorter duration, than estimated here. Alternatively, they may suggest a relatively weak overturning circulation at the Palaeocene–Eocene boundary, as seen in some dynamical ocean/atmosphere models¹⁹. Our model can replicate the magnitude of the observed recovery only if we assume that POE recovery nodules formed in soils where a high proportion of subsurface CO_2 was derived from the atmosphere. This is consistent with the occurrence of these nodules in relatively coarse-grained, poorly developed palaeosols. In contrast to the short-lived POE, low $\delta^{13}\text{C}$ values were sustained for >90 kyr during the CIE ‘body’ (between 118 and 74 MCD in the BBCP record), perhaps indicating crossing of climatic or biogeochemical thresholds supporting sustained changes during the main body of the PETM, but not the POE (ref. 20). Our simulations do not fully replicate the very low soil carbonate $\delta^{13}\text{C}$ values of the CIE body, suggesting that this threshold event may have involved changes in soil properties (for example, seasonality of soil carbonate formation, soil permeability, short-term respiration rates) that reduced subsurface $\delta^{13}\text{C}$ values beyond those in the model.

Our data favour primary PETM carbon input mechanisms that could produce repeated, catastrophic releases to the atmosphere and surface ocean at high rates. Several proposed models do not satisfy these constraints, either because the triggering mechanism is unique (for example, bolide impacts²¹), or because they release carbon at relatively low rates (for example, seaway desiccation²², permafrost oxidation²³). Recent evidence for extremely rapid PETM C release that has been suggested to support an impact trigger for the event³ is derived from a short marine-margin record, which may truncate evidence for the POE. Our data indicate two, $\sim 10^3$ -year-long C release events at the PETM onset and are thus inconsistent with bolide impact as the sole PETM C release mechanism.

Models involving massive methane release in response to discrete regional events (for example, volcanic intrusion and thermogenic methane release²⁴, seafloor slumping and methane clathrate release²⁵) are more easily reconciled with our results. In particular, we note that the approximate length of time separating the POE and CIE in the BBCP record is similar to that estimated for the propagation of a thermal pulse to hydrate-bearing depths in seafloor sediments²⁶, and suggest that carbon release during the CIE may

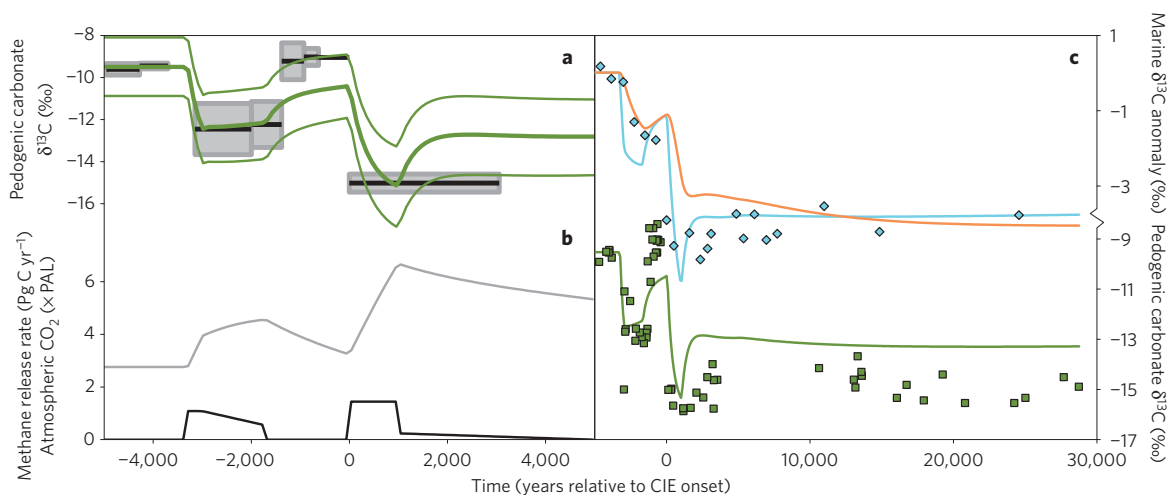


Figure 3 | Carbon-cycle change during the PETM onset. **a**, Observed and modelled pedogenic carbonate $\delta^{13}\text{C}$ (black lines: mean of each carbonate zone, grey boxes: $\pm 1\sigma$, green curves: model). Models have pre-PETM soil P_{CO_2} of 3,300 (thick curve), 2,600 (upper curve) and 4,500 (lower curve) ppmv. **b**, Prescribed rates of carbon release from methane (black); modelled atmospheric P_{CO_2} (grey; PAL = pre-industrial atmospheric level). **c**, Observed and modelled $\delta^{13}\text{C}$ (blue diamonds: dinocysts¹⁵; green squares: pedogenic carbonate (this study); blue curve: modelled surface ocean dissolved inorganic carbon; orange curve: modelled continental shelf surface sediments; green curve: intermediate model from **a**). See Supplementary Information for age models.

have been a feedback to warming generated by an initial release during the POE. If this is the case, the PETM may provide geologic evidence for a strong clathrate feedback to global warming at $\sim 10^3$ -year timescales, meaning that the long-term response of clathrates to anthropogenic warming deserves further consideration²⁷.

All model scenarios that match our observations require relatively high carbon release rates, of the order of 1 Pg yr^{-1} , at the beginning of the PETM, even though our simulations assume a relatively ^{13}C -depleted carbon source (-55%) that limits the amount of carbon required to explain the POE and CIE (Fig. 3 and Supplementary Fig. 13b). Our results are sensitive to modelling assumptions, and could be a factor of roughly two lower or many times higher if the model boundary conditions are incorrect or the isotopic composition of the added carbon differed from that assumed (Supplementary Information). Thus, the BBCP record suggests that rates of release during the PETM were probably within an order of magnitude of, and may have approached, the 9.5 Pg yr^{-1} associated with modern anthropogenic carbon emissions⁵. The rates and pattern of release inferred here are consistent with evidence from single-specimen analysis of foraminiferal tests²⁸, but contrast with much lower rates ($<0.3 \text{ Pg yr}^{-1}$) and continuous release inferred from methane-release simulations tuned to marine-margin records⁴ that may be affected by time-averaging⁹. Thus, our findings re-establish the possibility that the PETM may be a strong analogue for anthropogenic global change in terms of both magnitude and rates of change. Further constraints on the source of C released during the event and on the duration of the POE and CIE carbon pulses will be required to refine our understanding of these events and assess the degree to which changes in global temperatures, ocean pH, and terrestrial plant and animal communities during the PETM (ref. 2) are an appropriate model for Earth's future.

Methods

Data reported in this paper are available in the Supplementary Information and archived at <http://doi.pangaea.de/10.1594/PANGAEA.817119>.

Received 29 May 2014; accepted 10 November 2014;
published online 15 December 2014

References

1. Westerhold, T., Röhl, U. & Laskar, J. Time scale controversy: Accurate orbital calibration of the early Paleogene. *Geochim. Geophys. Geosyst.* **13**, Q06015 (2012).
2. McInerney, F. A. & Wing, S. L. The Paleocene–Eocene thermal maximum: A perturbation of carbon cycle, climate, and biosphere with implications for the future. *Annu. Rev. Earth Planet. Sci.* **39**, 489–516 (2011).
3. Wright, J. D. & Schaller, M. F. Evidence for a rapid release of carbon at the Paleocene–Eocene thermal maximum. *Proc. Natl Acad. Sci. USA* **110**, 15908–15913 (2013).
4. Cui, Y. *et al.* Slow release of fossil carbon during the Palaeocene–Eocene thermal maximum. *Nature Geosci.* **4**, 481–485 (2011).
5. Ciais, P. *et al.* in *Climate Change 2013: The Physical Science Basis* (eds Stocker, T. F. *et al.*) 465–570 (IPCC, Cambridge Univ. Press, 2013).
6. Kraus, M. J. & Gwinn, B. Facies and facies architecture of Paleogene floodplain deposits, Willwood Formation, Bighorn Basin, Wyoming, USA. *Sed. Geol.* **114**, 33–54 (1997).
7. Bowen, G. J. *et al.* in *Paleocene–Eocene Stratigraphy and Biotic Change in the Bighorn and Clarks Fork Basins, Wyoming* (ed. Gingerich, P. D.) 73–88 (Univ. of Michigan Museum of Paleontology, 2001).
8. Cerling, T. E. The stable isotopic composition of modern soil carbonate and its relationship to climate. *Earth Planet. Sci. Lett.* **71**, 229–240 (1984).
9. Sluijs, A., Zachos, J. C. & Zeebe, R. E. Constraints on hyperthermals. *Nature Geosci.* **5**, 231 (2012).
10. Kirtland Turner, S. & Ridgwell, A. Recovering the true size of an Eocene hyperthermal from the marine sedimentary record. *Paleoceanography* **28**, 700–712 (2013).
11. Schneider-Mor, A. & Bowen, G. J. Coupled and decoupled responses of continental and marine organic-sedimentary systems through the Paleocene–Eocene thermal maximum, New Jersey margin, USA. *Paleoceanography* **28**, 105–115 (2013).

12. Clyde, W. C. *et al.* Basin-wide magnetostratigraphic framework for the Bighorn Basin, Wyoming. *Geol. Soc. Am. Bull.* **119**, 848–859 (2007).
13. Murphy, B. H., Farley, K. A. & Zachos, J. C. An extraterrestrial ^3He -based timescale for the Paleocene–Eocene thermal maximum (PETM) from Walvis Ridge, IODP Site 1266. *Geochim. Cosmochim. Acta* **74**, 5098–5108 (2010).
14. Secord, R., Gingerich, P. D., Lohmann, K. C. & MacLeod, K. G. Continental warming preceding the Palaeocene–Eocene thermal maximum. *Nature* **467**, 955–958 (2010).
15. Sluijs, A. *et al.* Environmental precursors to rapid light carbon injection at the Palaeocene/Eocene boundary. *Nature* **2007**, 1218–1222 (2007).
16. Self-Trail, J. M., Powars, D. S., Watkins, D. K. & Wandless, G. A. Calcareous nannofossil assemblage changes across the Paleocene–Eocene Thermal Maximum: Evidence from a shelf setting. *Mar. Micropaleontol.* **92**, 61–80 (2012).
17. Zachos, J. C. *et al.* Rapid acidification of the ocean during the Paleocene–Eocene thermal maximum. *Science* **308**, 1611–1615 (2005).
18. Bains, S., Corfield, R. M. & Norris, R. D. Mechanisms of climate warming at the end of the Paleocene. *Science* **285**, 724–727 (1999).
19. Winguth, A. M. E. in *Climate Change–Geophysical Foundations and Ecological Effects* Vol. 1 (eds Blanco, J. & Kheradmand, H.) 43–64 (IntTech, 2011).
20. Bowen, G. J. Up in smoke: A role for organic carbon feedbacks in Paleogene hyperthermals. *Glob. Planet. Change* **109**, 18–29 (2013).
21. Cramer, B. S. & Kent, D. V. Bolide summer: The Paleocene/Eocene thermal maximum as a response to an extraterrestrial trigger. *Palaeogeogr. Palaeoclimatol. Palaeoecol.* **224**, 144–166 (2005).
22. Higgins, J. A. & Schrag, D. P. Beyond methane: Towards a theory for the Paleocene–Eocene thermal maximum. *Earth Planet. Sci. Lett.* **245**, 523–537 (2006).
23. DeConto, R. *et al.* Past extreme warming events linked to massive carbon release from thawing permafrost. *Nature* **484**, 87–92 (2012).
24. Svensen, H. *et al.* Release of methane from a volcanic basin as a mechanism for initial Eocene global warming. *Nature* **429**, 542–545 (2004).
25. Katz, M. E., Pak, D. K., Dickens, G. R. & Miller, K. G. The source and fate of massive carbon input during the latest Paleocene thermal maximum. *Science* **286**, 1531–1533 (1999).
26. Zeebe, R. E. What caused the long duration of the Paleocene–Eocene Thermal Maximum? *Paleoceanography* **28**, 440–452 (2013).
27. Archer, D. Methane hydrate stability and anthropogenic climate change. *Biogeosciences* **4**, 521–544 (2007).
28. Thomas, D. J., Zachos, J. C., Bralower, T. J., Thomas, E. & Bohaty, S. Warming the fuel for the fire: Evidence for the thermal dissociation of methane hydrate during the Paleocene–Eocene thermal maximum. *Geology* **30**, 1067–1070 (2002).
29. Gingerich, P. D. in *Paleocene–Eocene Stratigraphy and Biotic Change in the Bighorn and Clarks Fork Basins, Wyoming* Vol. 33 (ed. Gingerich, P. D.) 37–71 (Univ. of Michigan Papers on Paleontology, 2001).
30. Aziz, H. A. *et al.* Astronomical climate control on paleosol stacking patterns in the upper Paleocene–lower Eocene Willwood Formation, Bighorn Basin, Wyoming. *Geology* **36**, 531–534 (2008).

Acknowledgements

This research used samples and/or data provided by the Bighorn Basin Coring Project (BBCP), and we thank the BBCP Science Team for participation in core collection, processing and sampling. We are grateful to H. Kuhlmann, H.-J. Wallrabe-Adams, L. Schnieders, V. Lukies, A. Wülbers and W. Hale for their assistance throughout the project. We are indebted to R. Wilkens for providing knowledge and access to image analysis procedures. We thank V. Srinivasaraghavan, J. VanDeVelde, B. Theiling and S. Chakraborty for assistance with laboratory analyses. Funding for this research was provided by United States National Science Foundation grants 0958821, 0958622, 0958583 and 1261312, and by the Deutsche Forschungsgemeinschaft.

Author contributions

G.J.B., B.J.M., P.D.G., W.C.C. and S.L.W. designed the study. B.J.M. carried out isotopic and petrographic analyses. U.R., T.W. and P.D.G. developed the composite depth scale, assembled the core images, and established the correlation to the outcrop level. M.J.K. developed the age model. A.S. collected data on carbonate nodule occurrence and morphology. G.J.B. developed and ran the carbon-cycle model simulations. G.J.B. and B.J.M. wrote the manuscript. All authors reviewed the manuscript and contributed to the Supplementary Information.

Additional information

Supplementary information is available in the [online version of the paper](#). Reprints and permissions information is available online at www.nature.com/reprints. Correspondence and requests for materials should be addressed to G.J.B.

Competing financial interests

The authors declare no competing financial interests.